MEDFARM: Jurnal Farmasi dan Kesehatan, Vol.14, No.2, 2025, Page 666-685
e-ISSN : 2715-9957
p-ISSN: 2354-8487

Computational Investigation of α-Glucosidase Inhibition by Phytochemical Compounds from *Muntingia calabura* L. Leaves: Insights into Potential Antidiabetic Agents

Syaiful Prayogi[1*], Aulia Rahman[2], Tsaniatul Mahbubah[3], Nabilla Defira Putri Maisaan[4]

[1,2,3,4)] Bachelor of Pharmacy Study Program, Faculty of Science and Technology, University of Peradaban, Indonesia

e-mail:
syiafulprayogimfarm@gmail.com

ABSTRACT

Diabetes Mellitus (DM) is a degenerative disease that poses a major global health problem. It is characterized by increased blood glucose levels (hyperglycemia). Common therapeutic agents for DM include sulfonylureas, biguanides, and α-glucosidase inhibitors. However, the use of α-glucosidase inhibitors is often associated with several issues such as the presence of non-intestinal α-glucosidase in various body cells, gastrointestinal side effects (diarrhea, bloating, abdominal discomfort), and high IC_{50} values indicating low potency and efficacy against the α-glucosidase enzyme. This study aims to explore the potential of flavonoid compounds from *Muntingia calabura* L. (kersen) leaves as α-glucosidase inhibitors through in silico analysis. The study was conducted using molecular docking to evaluate the binding affinity and interaction of flavonoid compounds with the α-glucosidase enzyme. The docking results showed that 8 ligands test exhibited strong binding affinities, inhibitors constants, and stable interactions with the active site of α-glucosidase, comparable to standard inhibitors (acarbose). The two most effective candidate ligands for α-glucosidase inhibition were 20,4′-dihydroxy-3′-methoxydihydrochalcone (502) and (−)-3′-methoxy-2′,4′, β-trihydroxydihydrochalcone (513). These compounds demonstrated binding affinities of −7.33 and −7.30 kcal/mol with inhibition constants of 4.27 and 4.45 μM, respectively, indicating strong potential as natural α-glucosidase inhibitors and promising lead molecules for developing new antidiabetic agents. Their inhibitory potential was further supported by favorable ADMET parameters and alignment with Lipinski's rule of five. Additional in vitro and in vivo investigations are required to validate these results.

Keywords: antidiabetic, *Muntingia calabura* L., α-glucosidase inhibitor, molecular docking

Introduction

Diabetes Mellitus (DM) is a degenerative disorder that remains a major global health concern. It is characterized by elevated blood glucose levels or hyperglycemia (Perkeni, 2015) and is closely associated with several complications, including cardiovascular diseases (Fiorentino et al., 2013). Based on insulin deficiency, DM is classified into two major types: type 1 and type 2. According to the

International Diabetes Federation (IDF) report in 2019, approximately 463 million people worldwide are living with DM, and this number is projected to increase to 13.7 million by 2030 and 16.9 million by 2045 (Atlas, 2019; Yang et al., 2020).

The current treatment of DM, particularly type 2 DM, relies mainly on synthetic drugs that often cause adverse effects. Commonly used drug classes include sulfonylureas, biguanides, and α-glucosidase inhibitors (Padhi et al., 2020). α-Glucosidase inhibitors, administered orally, act by delaying carbohydrate digestion in the intestine, thereby preventing postprandial hyperglycemia. However, some of these drugs are absorbed and inhibit non-intestinal α-glucosidase present in various body cells, which can lead to undesirable side effects (Reuse & Wisselaar, 1994). Hence, the discovery of safer and more effective antidiabetic agents is urgently needed.

The conventional drug development process is time-consuming (10–15 years) and costly, with only one out of approximately 10,000 candidates typically reaching the market due to pharmacokinetic limitations and toxicity issues during clinical trials (DiMasi et al., 2016). With advancements in computational technology, *structure-based virtual screening* methods such as *molecular docking* have become efficient alternatives in drug discovery (Ma et al., 2013). This approach allows early elimination of compounds with low drug-likeness, thereby reducing cost and improving efficiency.

Molecular docking provides insight into the optimal geometry of receptor–ligand complexes and binding energy, which can be used to predict the potential of a molecule as a drug candidate (Frimayanti et al., 2021). Moreover, in silico and in vitro methods are considered efficient due to their faster testing times, minimal sample requirements, and the absence of animal use (Ikrom et al., 2014).

Natural products remain an important source for drug discovery. One promising plant species is kersen (*Muntingia calabura* L.), which grows widely in Indonesia but remains underutilized. This plant contains various bioactive compounds with pharmacological potential, including flavonoids (Laswati, 2018). Tahir M. et al. (2022) reported that ethanolic extracts of *M. calabura* flowers contain several classes of flavonoids such as flavonols, flavanones, and anthocyanidins (Tahir et al., 2022). Additionally, antioxidant testing of methanolic extracts using the DPPH radical scavenging method yielded an IC_{50} value of 9.271 µg/mL, indicating very strong antioxidant activity (Sami et al., 2017). Other studies have also reported the plant's antidiabetic and antioxidant properties (Rahmadani et al., 2022).

Flavonoids are known α-glucosidase inhibitors that function by reducing glucose absorption in the small intestine, thereby lowering blood glucose levels (Sinulingga et al., 2020). Mahmood et al. (2014) identified numerous flavonoid compounds in *M. calabura* leaves, including (2R,3R)-7-methoxy-3,5,8-trihydroxyflavanone, pinocembrin, chrysin, galangin, and other flavonol and flavanone derivatives with potential biological activity(Mahmood et al., 2014a)..

Based on these findings, this study aims to explore the α-glucosidase inhibitory activity of constituent compounds in kersen *Muntingia calabura* L. leaves through an in silico approach using *molecular docking* analysis.

Methodology

The computational study was performed using a personal computer with the following specifications: Intel® Core™ i5-10400 CPU @2.9 GHz (12 cores), 8 GB DDR4 RAM, and an NVIDIA GeForce 210 graphics card. The analyses were further supported by a secondary system running Windows 10 64-bit operating system.

Several software applications were employed throughout the research process. Biovia Discovery Studio 2021 (BDS 2021) was used for protein and ligand preparation as well as visualization of docking interactions. PyMOL was utilized for RMSD validation, PyRx 0.8 for molecular docking simulations, and Chemsketch for constructing 2D and 3D molecular structures. Additionally, SWISSADME and ADMETLab 3.0—both web-based platforms—were applied to predict pharmacokinetic and toxicity profiles (ADMET parameters) of the selected compounds. Microsoft Excel package was used for simple data analysis.

Preparation of Target Protein and Ligands

All chemical constituents identified in *Muntingia calabura L.* (kersen) leaves were sketched using Chemsketch and subsequently saved as *.mol* files. The target protein, α-glucosidase (PDB ID: 5NN8) (Rehman et al., 2019), was prepared by removing all water molecules and separating the native ligand using Discovery Studio Visualizer (DSV). The processed protein structure was then saved in *.pdb* format (Huey et al., 2012).

Docking Validation

Validation of the docking protocol was carried out by redocking the native ligand into the α-glucosidase active site. The procedure was deemed reliable when the Root Mean Square Deviation (RMSD) between the predicted pose and the crystallographic orientation of the ligand was ≤ 2 Å (Istyastono, 2018). The RMSD thresholds are interpreted as follows: values ≤ 1 Å indicate an excellent alignment that closely replicates the native conformation; 1 Å < RMSD ≤ 2 Å reflects a good pose that still approximates the native structure; 2 Å < RMSD ≤ 3 Å suggests a conformation with noticeable deviations; and RMSD > 3 Å denotes a poor fit. Additionally, the key amino acid residues engaged in binding, along with the types of intermolecular interactions formed, should correspond closely to those observed in the original crystal complex (Sari et al., 2020).

Docking Procedure

The preprocessed protein and ligand structures were imported into pyRx for molecular docking simulations. Docking grid parameters and algorithmic settings were defined according to standard protocols. The resulting docking conformations were then visualized and analyzed using BDS (Khalil et al., 2020). All test compounds were docked against the α-glucosidase enzyme (PDB ID: 5NN8).

Visualization of Docking Results

Docking outcomes were visualized in both three-dimensional (3D) and two-dimensional (2D) formats to elucidate the intermolecular interactions between the ligand and the active site residues of the target protein. The visualization was carried out using BDS (Sari et al., 2020).

Evaluation of Docking Results

The docking results were assessed based on binding energy, inhibition constanta, amino acid interactions, and intermolecular bonding patterns between the test ligands and the α-glucosidase enzyme. Lower binding energy values indicate a more stable ligand–protein complex (Manna et al., 2017). Detailed visual representations of the ligand–protein interactions were generated in both 2D and 3D formats using BDS.

ADMET Profile Prediction

The Absorption, Distribution, Metabolism, Excretion, and Toxicity (ADMET) profiles of the investigated compounds were estimated in silico using the online resources available at *SwissADME* and *ADMETlab 3.0*. These platforms provide comprehensive evaluations of physicochemical parameters, lipophilicity, aqueous solubility, pharmacokinetic behavior, drug-likeness, and potential toxicity. For each molecule, its SMILES notation was submitted into the corresponding prediction modules to generate the ADMET assessments**.**

Result and Discussion

Despite several reports on α-glucosidase inhibition by phytochemicals, including flavonoids and other natural compounds, most existing studies either focus on isolated constituents from medicinal plants or rely predominantly on *in vitro* enzyme assays with limited computational analysis. For example, prior work on *Muntingia calabura* leaves isolated flavones that exhibited α-glucosidase inhibition and assessed their binding through docking and molecular dynamics simulations, emphasizing structure–activity relationships (SAR) (Nguyen et al., 2025). Similarly, other computational investigations have identified putative inhibitors from Nigerian antidiabetic plants or various medicinal extracts against carbohydrate-digesting enzymes, integrating docking and ADMET profiling (Ogboye et al., 2022). However, these studies have not comprehensively characterized the specific phytochemical derivatives from *M. calabura* leaves through a combined pipeline of high-resolution docking, ADMET prediction, and drug-likeness evaluation, nor have they contextualized their findings within detailed pharmacokinetic and toxicity predictions. The present study fills this gap by computationally evaluating novel *M. calabura* compounds against α-glucosidase with integrated ADMET and drug-likeness profiling, thereby providing a more holistic in silico assessment of both binding potential and pharmacological suitability that extends beyond affinity scoring alone. Summary of Related Studies on α-Glucosidase Inhibitors from Natural Products show in Table 1.

Table 1. Summary of Related Studies on α-Glucosidase Inhibitors from Natural Products

Study (Year)	**Source of Compounds**	**Target Protein**	**Methodology**	**Key Findings**	**Research Gap**
Onyegbule et al. (2022)	Nigerian antidiabetic plants	α-Glucosidase, α-Amylase	Molecular docking, ADMET prediction	Identified several natural compounds with favorable binding affinities and acceptable ADMET profiles	Did not focus on *Muntingia calabura*; no detailed drug-likeness or comparative lead optimization
Nguyen et al. (2025)	*Muntingia calabura* leaves (isolated flavones)	α-Glucosidase	In vitro enzyme inhibition, docking, SAR analysis	Flavones showed significant inhibitory activity and key residue interactions	Limited pharmacokinetic/toxicity profiling; no comprehensive ADMET or drug-likeness assessment
(Lam et al., 2024)	*Flavonoids from various natural sources*	α-Glucosidase & α-Amylase	Systematic review of in vitro studies; SAR analysis	Identified hundreds of flavonoid structures with dual inhibitory effects against both enzymes; highlighted structural features for activity	Focuses on flavonoids broadly; does not evaluate comprehensive ADMET or drug-likeness, nor specific computational profiling for individual compounds investigated in current study (e.g., Muntingia calabura derivatives) (Springer Link)
(Deng et al., 2025)	*A broad spectrum of natural products (flavonoids, terpenes, alkaloids, phenols, chalcones, etc.)*	α-Glucosidase	Review of chemical diversity & bioactivity of plant/microbe-derived inhibitors	Classified 139 distinct natural compounds into structural groups with α-glucosidase inhibition; many exhibit promising bioactivity	Does not integrate computational predictions (docking/ADMET) or focus on specific phytochemical sources such as Muntingia calabura leaves; lacks holistic pharmacokinetic evaluation (PubMed)
Pires et al. (2015)	Drug-like small molecules	Multiple targets	pkCSM-based ADMET modeling	Established ADMET criteria for oral drug candidates(Pires et al., 2015)	Methodological focus only; not applied to *M. calabura* phytochemicals
Present work	***Muntingia calabura* leaf phytochemicals**	**α-Glucosidase**	**Integrated docking, ADMET, drug-likeness, toxicity profiling**	**Identifies promising antidiabetic candidates with balanced affinity and pharmacokinetics**	**Addresses lack of holistic in silico evaluation for *M. calabura*-derived compounds**

Preparation of Target Protein and Ligands

A total of nine test ligands derived from *Muntingia calabura* and the reference ligand (acarbose) are presented in Table 1**.** The target protein employed in this study was human lysosomal acid α-glucosidase (GAA)**.** GAA is an enzyme responsible for catalyzing the hydrolysis of glycogen—a complex carbohydrate—into glucose within the lysosome, an organelle functioning as the cellular recycling center (Roig-Zamboni et al., 2017). The structure of the target protein is illustrated in Figure 1**.**

MEDFARM: Jurnal Farmasi dan Kesehatan, Vol.14, No.2, 2025, Page 666-685
e-ISSN : 2715-9957
p-ISSN: 2354-8487

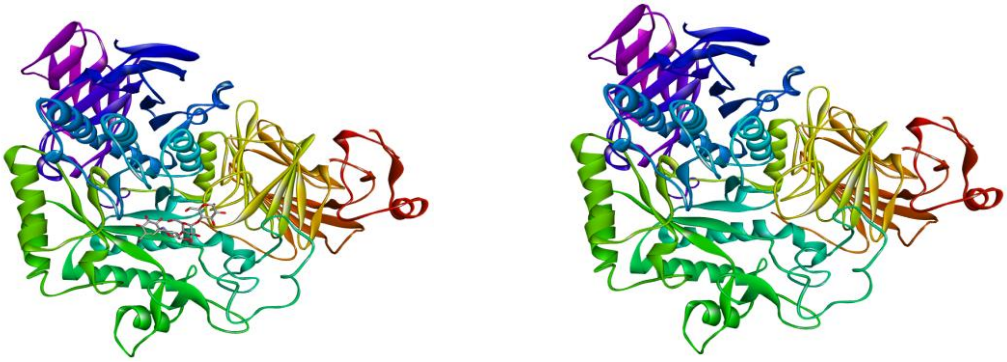

A B

Figure 1. Target protein**.** Binding position of acarbose (A); native target protein (B).

Table 1. Structure of ligands test (base on reference (Mahmood et al., 2014b))

Ligand name-(code)	Structure
(2R,3R) 7 Methoxy 3,5,8 trihydroxyflavanone-(131)	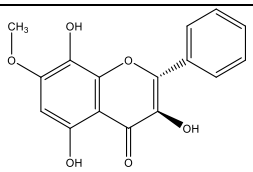
20,40 Dihydroxy 30 methoxydihy drochalcone-(502)	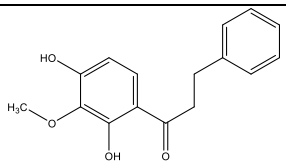
(-) 30 Methoxy 20,40,b-trihydrox-ydihydrochalcone-(513)	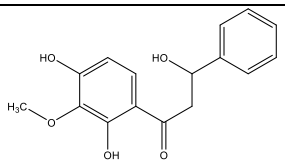
(2S) (-) 50 Hydroxy 7,30,40-tri-methoxyflavanone-(524)	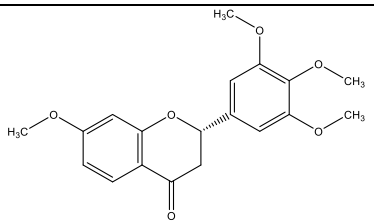
8 hydroxy 10 methoxy 5H iso chromeno[4,3-b]chromen 7 one (muntingone)-(535)	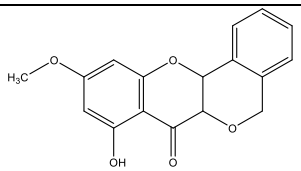
2,3-Dihydroxy-4,30,40,50-tetra-methoxydihydrochalcone-(656)	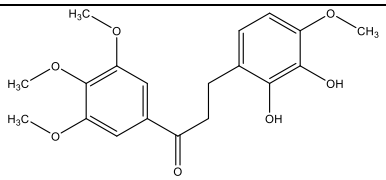

Ligand name-(code)	Structure
4,20,40-Trihydroxy-30-methoxydi-hydrochalcone-(667)	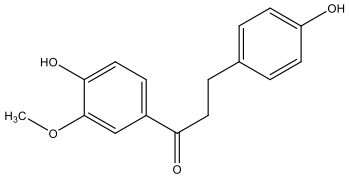
(2R,3R) (-) 3,5 Dihydroxy 6,7 dimethoxyflavanone-(678)	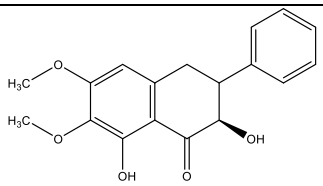
8 Hydroxy 6 methoxyflavone (calaburone)-(879)	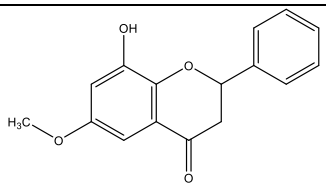
Acarbose (ref)	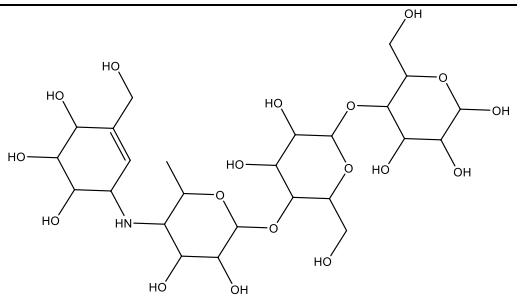

Docking (Validation and Procedure)

Docking validation was performed using a grid box centered at x = –13.4, y = –38.2, and z = 94.9, which produced an RMSD of 1.5016 Å. This procedure, illustrated in Figure 2, consisted of re-docking the reference ligand (acarbose) into the enzyme's active site. The docking protocol was deemed reliable because the RMSD value met the ≤ 2 Å criterion (Al Azzahra et al., 2024).. As depicted in Figure 2, the amino acid residues interacting with the co-crystallized and re-docked ligands showed strong correspondence. These validated parameters were subsequently applied for the docking of the test ligands.

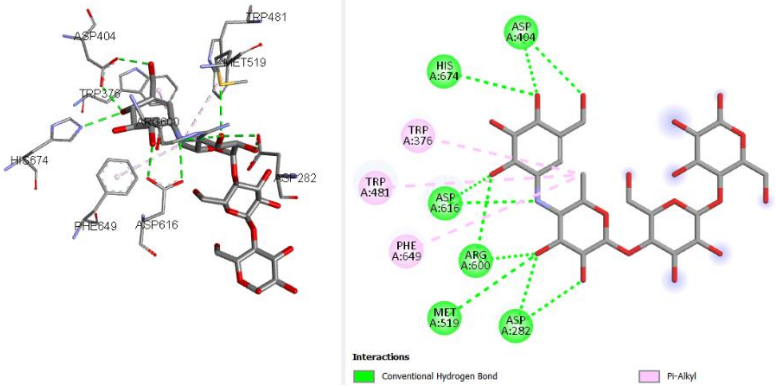

A

MEDFARM: Jurnal Farmasi dan Kesehatan, Vol.14, No.2, 2025, Page 666-685
e-ISSN : 2715-9957
p-ISSN: 2354-8487

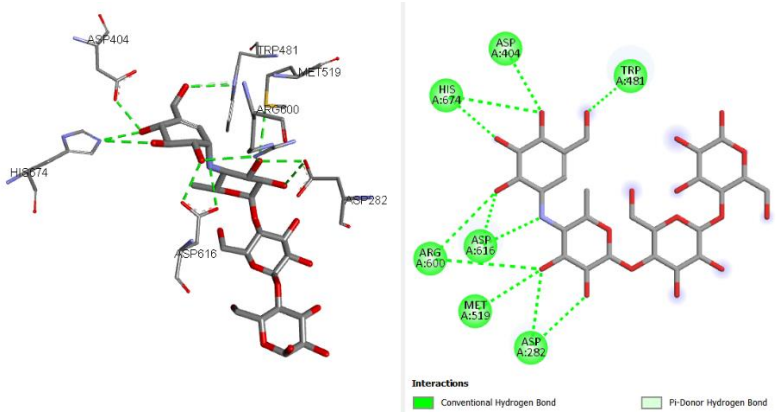

B

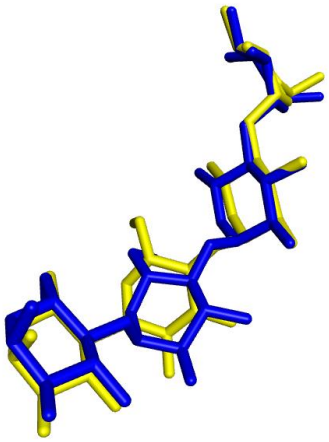

C

Figure 2. Visualization of docking validation results**.** Interaction of the co-crystal (A); interaction of the re-docking (B); superimposition of the acarbose ligand — yellow: co-crystal, blue**:** re-docking (C).

Docking of the Test Ligands

Based on the molecular docking analysis of the test ligands against the target protein, all compounds exhibited more favorable binding affinities and lower inhibition constants (Ki) compared to the reference ligand, acarbose. Only compound 52 ((2S)- (-)- 5′- Hydroxy- 7,3′,4′- trimethoxyflavanone) displayed a higher binding affinity value and inhibition constant, as presented in Table 2. Among the tested ligands, compounds 502 and 513 demonstrated the most promising inhibitory activity, with Ki values of 4.27 µM and 4.45 µM, respectively, and comparable binding affinities of approximately −7.3 kcal/mol. These two compounds were therefore selected for further interaction visualization and analysis, as illustrated in Figure 3 and Table 3.

The inhibitory potential of a ligand toward a receptor can be evaluated through its inhibition constant (Ki), which is closely related to binding affinity. A smaller Ki value indicates a stronger binding affinity and a lower concentration of ligand required to effectively inhibit the enzyme's activity. In other words, the smaller the Ki, the stronger the ligand–protein interaction (Klebe, 2013).

Visualization and interaction analysis from the docking results were conducted to validate and compare the binding conformations between the reference

ligand (acarbose) and the test ligands (Figure 3). Ligand 20,40 Dihydroxy 30 methoxydihydrochalcone-(code:502) exhibited similar amino acid residue interactions to acarbose, involving HIS A:674, ARG A:600, ARG A:518, ASP A:404, ASP A:616, and PHE A:649, forming both hydrogen bonds and hydrophobic interactions (Table 3). These findings suggest that these residues play a crucial role in ligand binding and contribute significantly to the α-glucosidase inhibitory activity.

The visualization also reveals how active-site amino acid residues engage with the docked ligands. These residues mediate key non-covalent interactions—such as hydrogen bonds, hydrophobic contacts, and electrostatic forces—that collectively govern the stability and affinity of the ligand–protein complex (Karim et al., 2023).

Table 2. Docking results of the test ligands

Ligands	Binding Affinity (kcal/mol)	Ki (μM)
502	-7.33	4.27
513	-7.30	4.45
678	-7.20	5.27
879	-7.10	6.24
131	-7.10	6.24
667	-6.85	9.51
656	-6.73	11.75
535	-6.60	14.51
ref	-6.15	31.01
524	-5.85	51.46

Binding affinity energy serves as an indicator of the stability of the ligand–protein complex and represents a critical characteristic determining drug efficacy. Lower (more negative) binding energy values indicate a more favorable and spontaneous interaction between the ligand and its target (Prayogi et al., 2023). Base on Table 2. ligand 502 exhibited the lowest binding energy, indicating a stable and spontaneous binding interaction with the target.

Table 3. **Amino acid residue interaction profile with the test ligands**

Ligands	Binding Affinity (kkal/mol)	Ki (μm)	Amino Acid	Bond Type
502	-7.33	4.27	**HIS A:674**	Hydrogen bond, hydrophobic bond
			ARG A:600	Hydrogen bond
			ARG A:518	Hydrogen bond
			ASP A:404	Hydrogen bond
			ASP A:616	Hydrogen bond
			TRP A:613	Hydrophobic bond
			PHE A:649	Hydrophobic bond
			TRP A:613	Hydrophobic bond
			ASP A:518	Electrostatic bond

513	-7.30	4.45	**ARG A:600**	Hydrogen bond
			ARG A:518	Hydrogen bond
			ASP A:616	Hydrogen bond
			TRP A:516	Hydrophobic bond
			HIS A:674	Hydrophobic bond
			TRP A:516	Hydrophobic bond
			ASP A:518	Electrostatic bond
ref	-6.15	31.01	**ASP A:404**	Hydrogen bond
			HIS A:674	Hydrogen bond
			ASP A:616	Hydrogen bond
			ARG A:600	Hydrogen bond
			MET A:519	Hydrogen bond
			ASP A:282	Hydrogen bond
			TRP A:376	Hydrophobic bond
			TRP A:481	Hydrophobic bond
			PHE A:649	Hydrophobic bond

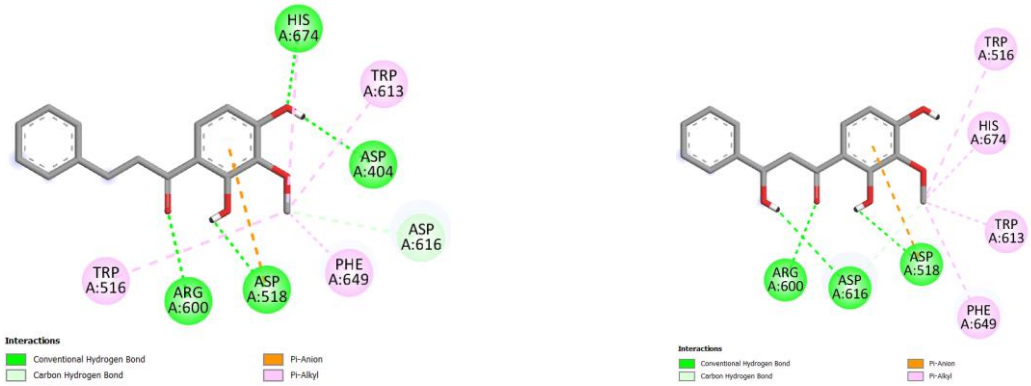

A **B**

Figure 3. Visualization of interactions between the ligands and the target protein. 20,40-Dihydroxy-30-methoxydihydrochalcone (502) [A] and (–)-30-Methoxy-20,40, β-trihydroxydihydrochalcone (513) [B].

ADMET Profile Prediction

Absorption

Absorption refers to the process by which an active compound is transported from its site of administration into the systemic circulation. Several predictive parameters are commonly employed to assess this process, including permeability assessments using human colon adenocarcinoma (Caco-2) cell models, as well as the parallel artificial membrane permeability assay (PAMPA), which evaluates the passive translocation of compounds intended for oral administration, promiscuous efflux transporter (P-glycoprotein; inhibitor/substrate) activity**,** human intestinal absorption (HIA)**,** and oral bioavailability (F)**.** These parameters collectively provide valuable insight into a compound's potential to achieve effective systemic exposure following oral administration.

Before an orally administered drug enters systemic circulation, it must traverse the intestinal epithelium, either by passive diffusion or transport-mediated mechanisms. The human colorectal adenocarcinoma cell line Caco-2 is widely employed as an in vitro model of this barrier because it differentiates into enterocyte-

like monolayers that closely mimic the structural and functional characteristics of human intestinal tissue. Consequently, Caco-2 permeability serves as a reliable predictive parameter for assessing a compound's potential to exhibit adequate intestinal absorption and systemic bioavailability**,** thereby representing a key criterion in the early evaluation of promising oral drug candidates.

The Parallel Artificial Membrane Permeability Assay (PAMPA) serves as an *in vitro* model designed to mimic the passive diffusion process of orally administered drugs across the gastrointestinal membrane. In this method, the stirring double-sink PAMPA system is employed to evaluate compound permeability driven by passive diffusion. The effective permeability coefficient (Peff) is typically reported in units of 10^{-6} cm/s**.** When integrated with complementary cell-based systems such as Caco-2 and Madin–Darby Canine Kidney cells (MDCK) models, PAMPA provides a more comprehensive assessment, helping to mitigate the limitations of individual models and thereby enhancing the predictive accuracy of a compound's intestinal absorption and membrane permeability in physiological conditions.

P-glycoprotein (P-gp), also known as MDR1 or ABCB1, is an ATP-binding cassette (ABC) transporter located within the cellular membrane. It is widely regarded as one of the most versatile xenobiotic efflux pumps, capable of recognizing and exporting a broad spectrum of structurally diverse compounds, many of which overlap with substrates of CYP3A4. Alterations in P-gp activity can markedly modify the pharmacokinetic behavior of P-gp substrate drugs, potentially yielding therapeutic advantages in specific situations while simultaneously introducing the risk of adverse drug interactions or clinical contraindications.

Human intestinal absorption (HIA) is a critical determinant of the pharmacological performance of orally administered agents. A well-established relationship exists between intestinal absorption and oral bioavailability, suggesting that HIA can, to a meaningful degree, function as a predictive indicator for estimating the oral bioavailability of a compound. Indeed, oral bioavailability remains one of the most critical pharmacokinetic determinants, as it reflects the overall efficiency of a drug's delivery into systemic circulation**,** thereby influencing its therapeutic performance and clinical effectiveness.

Table 4. Absorption Predictions

Absorption	Ligands			Interpretation
	502	513	acarbose	
Caco-2 Permeability	-4.93065	-5.09596	-7.04801	> -5.15: excellent (green); otherwise: poor (red)
PAMPA	0.112378	0.982687	1	A score within the range of 0–0.3 is interpreted as excellent and is denoted by a green category. Values between 0.3 and 0.7 indicate a moderate or intermediate level, represented by yellow. Scores falling between 0.7 and 1.0 reflect poor performance and are classified in the red category
Pgp-inhibitor	0.994383	0.007552	9.64E-09	
Pgp-substrate	0.00913	0.030414	0.999991	
HIA	0.013304	0.047274	0.99736	
F50%	0.965739	0.996584	0.999915	

The distribution characteristics of a compound are evaluated using several fundamental pharmacokinetic indicators, such as its degree of plasma protein binding (PPB), the human steady-state volume of distribution (VDss, Human), its ability to traverse the blood–brain barrier (BBB), and the proportion of the drug that remains unbound in plasma (Fu). These parameters collectively provide insight into how a compound is distributed throughout body compartments, its potential to cross biological barriers**,** and the extent to which it remains pharmacologically active in systemic circulation**.**

Table 5. Distribution Predictions

Distribution	**Ligands**			**Interpretation**
	502	**513**	**acarbose**	
PPB	98.28318	80.55913	15.88671	≤ 90%: excellent (green); otherwise: poor (red)
VDss	-0.63489	-0.28837	-0.52723	Values between 0.04 and 20 are classified as excellent (green), while all other values are considered poor (red)
BBB	0.026911	0.00387	1.36E-06	A score within the range of 0–0.3 is interpreted as excellent and is denoted by a green category. Values between 0.3 and 0.7 indicate a moderate or intermediate level, represented by yellow. Scores falling between 0.7 and 1.0 reflect poor performance and are classified in the red category
Fu	1.072436	19.71688	94.26575	>20%: High Fu; 5-20%: medium Fu; <5% low Fu

Metabolism is the process by which drug molecules undergo biotransformation into either active metabolite, capable of exerting pharmacological effects, or inactive metabolites, which are subsequently eliminated from the body. From a biochemical standpoint, Drug metabolism is generally divided into two major stages: Phase I reactions, which mainly consist of oxidative processes, and Phase II reactions, which encompass conjugation processes. In humans, cytochrome P450 (CYP) enzymes play a central role in metabolic transformation, with 57 known isozymes identified. Among these enzymes, CYP1A2, CYP3A4, CYP2C9, CYP2C19, CYP2D6, CYP2B6, and CYP2C8 represent the major catalysts of Phase I oxidative metabolism, with their activity primarily occurring in the liver. While CYP-mediated metabolism facilitates drug clearance, it can also result in the formation of toxic metabolites or trigger undesirable drug–drug interactions, which may compromise therapeutic safety.

The human liver microsomal (HLM) stability assay is one of the most widely employed *in vitro* approaches for evaluating the metabolic stability and hepatic clearance of chemical entities, reflecting the pivotal role of the liver as the primary organ involved in drug metabolism.

Table 6. Metabolism Predictions

Metabolism	**Ligands**			**Interpretation**
	502	**513**	**acarbose**	
CYP1A2 inhibitor	0.794285	0.3333580000	0.0000000002	

CYP1A2 substrate	0.970522	0.0007780000	0.0000000000	
CYP2C19 inhibitor	0.84988	0.0323370000	0.0000000000	
CYP2C19 substrate	0.173138	0.0156830000	0.0000000003	
CYP2C9 inhibitor	0.621272	0.1229930000	0.0000140000	
CYP2C9 substrate	0.649492	0.0006000000	0.0000073400	0: non-substrate/non-inhibitor; 1: substrate/inhibitor. The output represents the probability of a compound acting as a substrate or inhibitor, ranging from 0 to 1.
CYP2D6 inhibitor	0.079536	0.0004700000	0.0000276000	
CYP2D6 substrate	0.363798	0.0034850000	0.0000000000	
CYP3A4 inhibitor	0.919595	0.0205240000	0.0000000025	
CYP3A4 substrate	0.061912	0.9973290000	0.0000000058	
CYP2B6 inhibitor	0.000896	0.0000003290	0.0000141000	
CYP2B6 substrate	0.009685	0.0000000197	0.0000000000	
CYP2C8 inhibitor	0.99993	0.9064770000	0.9991800000	
HLM stability	0.990541	0.992975	0.128768	Values ranging from 0 to 0.3 indicate excellent performance (green), 0.3 to 0.7 represent moderate performance (yellow), and 0.7 to 1.0 correspond to poor performance (red).

Excretion refers to the process by which a drug is eliminated from the body, primarily through the renal pathway, where it is excreted in the urine. In addition to renal elimination, certain drugs may also be excreted via non-renal routes, including the lungs, skin, and various exocrine secretions such as sweat and saliva.

Among pharmacokinetic parameters, plasma clearance (CL_{plasma}) holds particular significance, as it determines the overall systemic exposure of a drug (for a given bioavailability) and serves as the key variable for calculating the maintenance dosage required to achieve steady-state plasma concentrations. CL_{plasma} represents the body's overall efficiency in eliminating a compound, defined as the rate of drug elimination (amount per unit time) relative to its plasma concentration. Empirically, clearance values are categorized as follows: >15 mL/min/kg for high clearance, 5–15 mL/min/kg for moderate clearance, and <5 mL/min/kg for low clearance.

The elimination half-life ($t_1/_2$) is a pharmacokinetic parameter that reflects both clearance and distribution volume. However, rather than relying solely on half-life, obtaining accurate and independent estimates of clearance and distribution volume provides a more meaningful understanding of a drug's elimination kinetics and dosing behavior in the body.

Table 7. Excretion Predictions

Excretion	Ligands			Interpretation
	502	513	Acarbose	

CL plasma	3.326015	2.728203	0.004697	0-5: excellent (green); 5-15: medium (yellow); > 15 : poor (red)
T1/2	1.169676	1.465936	3.813279	>8: excellent (green); 1-8: medium (yellow); <1 : poor (red)

Drug-induced neurotoxicity represents a frequently encountered adverse reaction, as numerous therapeutic agents and industrial chemicals are capable of disrupting neural function through multiple pathways. Such agents may injure both the central and peripheral nervous systems, producing neurological manifestations that may even mimic psychotic disorders. The severity of these neurotoxic effects ranges from transient and reversible disturbances to long-lasting, irreversible structural damage.

Ototoxicants constitute a class of substances capable of impairing the inner ear, either by directly damaging cochlear structures or by interfering with neural components involved in auditory processing.

Chemical-induced hematotoxicity refers to detrimental effects on hematopoietic tissues—including bone marrow—as well as on blood components such as platelets, leukocytes, and erythrocytes.

Drug-induced nephrotoxicity encompasses renal injury triggered by nephrotoxic compounds or medications, often resulting in rapid functional decline. The kidneys are particularly vulnerable to drug-related toxicity due to their high perfusion rate and their central role in the filtration and elimination of endogenous and exogenous substances. Proximal tubular cells, which participate in the concentration and reabsorption of glomerular filtrate, are especially susceptible to elevated intracellular levels of circulating toxicants. Consequently, drug-induced nephrotoxicity is recognized as a major causative factor in both acute kidney injury and chronic kidney disease.

Genotoxicity denotes the capacity of hazardous substances to alter or damage the genetic material of cells. Exposure to chemical or biological agents may induce genomic instability or epigenetic modifications, which can ultimately contribute to the onset of various diseases, including cancer.

The assessment of compound cytotoxicity is an essential component of early-stage drug discovery. The RPMI-8226 cell line, derived from multiple myeloma, is widely employed to evaluate the cytotoxic potential of investigational compounds. A549 cells, representing human non–small cell lung carcinoma, serve a similar purpose in evaluating toxicity toward lung-derived cancer cells. HEK293 cells, which originate from human embryonic kidney tissue, are known for their sensitivity to environmental perturbations and are frequently used in toxicity screening.

Drug-induced liver injury (DILI) continues to pose a major safety risk and is a primary reason for the withdrawal of drugs from the market. Hepatic toxicities identified during clinical development often force the discontinuation of drug candidates at advanced and costly stages. In DILI-related datasets, compounds with no association to hepatotoxicity keywords or adverse hepatic outcomes are labeled as non-hepatotoxic, while those with documented liver-related adverse reactions are

classified accordingly. Over the past five decades, DILI has been the predominant safety issue responsible for the removal of drugs from global markets. DILI-positive compounds include: (1) drugs withdrawn primarily due to hepatotoxicity, (2) agents not marketed in the United States because of hepatotoxic risks, (3) drugs assigned boxed warnings by the U.S. FDA, (4) marketed drugs carrying explicit hepatotoxicity warnings, and (5) older agents with numerous independent clinical reports (more than ten) linking them to liver injury. Compounds not meeting any of these criteria are categorized as DILI-negative.

Determining acute toxicity in mammalian models—such as rats or mice—constitutes a fundamental requirement in preclinical safety assessments of investigational drugs. The FDA Maximum (Recommended) Daily Dose is commonly used to estimate the human exposure level at which toxic effects may occur. Among toxicological endpoints, carcinogenicity is critical due to its serious health implications. Chemical-induced cancer may result from direct genomic damage or disruption of cellular metabolic processes. Some previously approved drugs were later recognized as carcinogenic in humans or animals and subsequently withdrawn. The Ames test is the most widely applied assay to assess mutagenicity, a key indicator of carcinogenic potential.

Based on Table 8, ligand 513 exhibits a lower toxicity potential—including drug-induced neurotoxicity, hematotoxicity, drug-induced nephrotoxicity, A549 cytotoxicity, HEK293 cytotoxicity, human hepatotoxicity, DILI, AMES mutagenicity, and acute oral toxicity in rats—compared with ligand 502.

Table 8. Toxicity Predictions

Toxicity	Ligands			Interpretation
	502	513	acarbose	
Drug induced neurotoxicity	0.574942	0.4954	0.000284	0: non; 1: yes The output value is the probability of being, within the range of 0 to 1.
Ototoxicity	0.230992	0.380207	0.999753	
Hematotoxicity	0.298458	0.073574	0.393946	
Drug induced Nephrotoxicity	0.501722	0.283774	0.97953	
Genotoxicity	0.223029	0.509623	0.031846	
RPMI-8226 Immunitoxicity	0.042508	0.046015	0.255018	
A549 Cytotoxicity	0.195282	0.074913	0.090745	
Hek293 Cytotoxicity	0.307791	0.157259	0.031315	
Human Hepatotoxicity	0.514926	0.21037	0.365764	
DILI	0.081559	0.014134	0.75619	
AMES Mutagenicity	0.338761	0.249734	0.906439	
Rat Oral Acute Toxicity	0.26853	0.176518	0.001156	
FDAMDD	0.312126	0.527851	0.001224	
Carcinogenicity	0.372012	0.386782	0.004066	

Lipinski's Rule of Five provides a foundational heuristic for anticipating whether a compound possesses the physicochemical attributes required to permeate cellular membranes through passive diffusion. This rule functions as an early filtering tool in drug discovery, helping researchers judge the drug-likeness of newly identified molecules. A compound is generally regarded as compliant with Lipinski's criteria

when it fulfills the following parameters: (1) a molecular weight under 500 Da; (2) a logP value of 5 or lower; (3) no more than five hydrogen bond donors; and (4) no more than ten hydrogen bond acceptors.

Beyond these classical benchmarks, additional physicochemical descriptors—such as molecular mass, lipophilicity (logP), aqueous solubility (logS), topological polar surface area (TPSA), the number of hydrogen bond donors and acceptors, synthetic accessibility, and structural resemblance to natural products—play an equally important role in defining and refining candidate molecules throughout the drug development pipeline.

Table 9. Drug Likenes Predictions

Physicochemical Chemical property/Drug Likenes	**Ligands**			**Interpretation**
	502	513	acarbose	
Promiscuous compounds	0.135	0.107	0.037	Category 0 denotes a compound that exhibits non-promiscuous behavior, whereas Category 1 refers to a compound classified as promiscuous. The predicted output represents the likelihood of belonging to either category and is expressed as a probability value ranging from 0 to 1.
Reactive compounds	0.736	0.429	0.093	
Lipinski Rule	0	0	1	Compounds that comply with the general thresholds of **molecular weight ≤ 500 Da**, **logP ≤ 5**, **no more than 10 hydrogen bond acceptors**, and **no more than 5 hydrogen bond donors** are considered to fall within the conventional physicochemical space associated with favorable oral bioavailability. **Interpretation of outcomes:** When **two physicochemical parameters fall outside** their recommended limits, the compound is likely to exhibit **suboptimal absorption or limited permeability**, whereas a **single deviation** is generally still regarded as tolerable. **Empirical classification:** Compounds with **fewer than two violations** are categorized as **excellent** (green), whereas those with **two or more deviations** are designated as having **poor** characteristics (red).
Molecular Weight	272.1	288.1	645.25	The optimal range is 100 to 600, as suggested by the Drug-Like Soft Rule.
logP	3.256419	2.400626	-4.50574	The estimated logP value for a compound is expressed as the logarithm of its molar concentration (log mol/L). Compounds exhibiting logP values within the interval of 0 to 3 log mol/L

				are regarded as falling within an acceptable or optimal range.
logS	-2.95822	-2.82322	0.364172	The estimated solubility of a compound is expressed as the logarithmic value of its molar concentration (log mol/L). Compounds exhibiting predicted solubility values between −4 and 0.5 log mol/L are regarded as falling within an acceptable range.
nHA	4	5	19	Represents the total number of oxygen and nitrogen atoms within a molecule. According to the Drug-Like Soft Rule, the preferred range for this parameter is approximately **0 to 12**
nHD	2	3	14	This parameter represents the total count of hydroxyl (–OH) and amine (–NH) groups within a molecule. According to the Drug-Like Soft Rule, an optimal range for this descriptor is generally considered to be between **0 and 7**
TPSA	66.76	86.99	321.17	The total value obtained by summing the tabulated surface contributions of polar functional fragments. An optimal range of 0–140 is generally recommended, consistent with the Veber rule.
Synth	1	2	5	A synthetic accessibility score (SAscore) of **6 or above** generally indicates that a molecule is **challenging to prepare**, whereas a score **below 6** suggests that the compound is **relatively straightforward to synthesize**.
NPscore	0.733	0.887	1.829	The resulting score generally falls within a scale of −5 to 5. A higher score indicates a greater likelihood that the compound possesses natural-product (NP) characteristics.

Based on the drug-likeness profiles (Table 9), both ligand 502 and ligand 513 exhibit favorable drug-like properties, fulfilling all specified parameters. Notably, ligand 502 demonstrates the highest synthetic accessibility, indicating that it is the easiest to synthesize among the evaluated compounds.

Conclusion

The ligand 2′,4′-dihydroxy-3′-methoxydihydrochalcone (502) emerged as one of the most promising α-glucosidase inhibitors, exhibiting amino acid residue interactions comparable to those of the reference compound, acarbose. This ligand demonstrated a binding affinity of −7.33 kcal/mol with an associated inhibition constant of 4.27 μM. Its interaction pattern closely resembled that of acarbose, indicating a similar binding mode. Furthermore, the predicted inhibitory potential

was supported by favorable absorption, distribution, metabolism, excretion, and toxicity (ADMET) profiles, along with satisfactory drug-likeness characteristics.

Declaration of Competing Interest

The authors declare that they have no competing interests

Acknowledgment

We gratefully acknowledge the Institute for Research and Community Service, University of Peradaban, for supporting this work through the 2025 Basic Research Funding Program.

Reference

Al Azzahra, Y., Taufik Septiyan Hidayat, & Syumillah Saepudin. (2024). Penambatan Molekul Senyawa Aktif Sirih (Piper Betle L) Terhadap Reseptor Hsv-1 Sebagai Kandidat Anti Herpes. *Pharmaceutical Science And Clinical Pharmacy*, *2*(1), 20–25. Https://Doi.Org/10.61329/Pscp.V2i1.22

Atlas, I. D. F. D. (2019). International Diabetes Federation. In *The Lancet* (Ninth Edit, Vol. 266, Issue 6881). International Diabetes Federation. Https://Doi.Org/10.1016/S0140-6736(55)92135-8

Deng, C., Zhang, N., Lin, H., Lu, W., Ding, F., Gao, Y., & Zhang, Y. (2025). Recent Progress On Natural A-Glucosidase Inhibitors Derived From The Plants And Microorganisms. *Current Medicinal Chemistry*, *32*(11), 2115–2141. Https://Doi.Org/10.2174/0109298673272908231115101520

Dimasi, J. A., Grabowski, H. G., & Hansen, R. W. (2016). Innovation In The Pharmaceutical Industry: New Estimates Of R&D Costs. *Journal Of Health Economics*, *47*, 20–33. Https://Doi.Org/10.1016/J.Jhealeco.2016.01.012

Fiorentino, T., Prioletta, A., Zuo, P., & Folli, F. (2013). Hyperglycemia-Induced Oxidative Stress And Its Role In Diabetes Mellitus Related Cardiovascular Diseases. *Current Pharmaceutical Design*, *19*(32), 5695–5703. Https://Doi.Org/10.2174/1381612811319320005

Frimayanti, N., Djohari, M., & Khusnah, A. N. (2021). Molekular Docking Senyawa Analog Kalkon Sebagai Inhibitor Untuk Sel Kanker Paru-Paru A549 (Molecular Docking For Chalcone Analogue Compounds As Inhibitor For Lung Cancer A549). *Jurnal Ilmu Kefarmasian Indonesia*, *19*(1), 87–95.

Huey, R., Morris, G. M., & Forli, S. (2012). Using Autodock 4 And Autodock Vina With Autodocktools: A Tutorial. *The Scripps Research Institute Molecular*, *December*, 32.

Ikrom, T.R., D. A., A., R. W., B, B. P., N., R. T., & . W. (2014). The In Vitro Study: Anti Aeromonas Hydrophila Of Ethanol Extract Of Kamboja Leaves (Plumeria Alba). *Jurnal Sain Veteriner*, *32*(1). Https://Doi.Org/10.22146/Jsv.5428

Istyastono, E. P. (2018). *Rancangan Obat Dan Penapisan Virtual Berbasis Struktur*. Sanata Dharma University Press.

Karim, B. K., Tsamarah, D. F., Zahira, A., Rosandi, N. F., Swarga, K. F., Aulifa, D. L., Elaine, A. A., & Sitinjak, B. D. P. (2023). In-Silico Study Of Active Compounds In Guava Leaves (Psidium Guajava L.) As Candidates For Breast Anticancer Drugs. *Indonesian Journal Of Biological Pharmacy*, *3*(3), 194–209. Https://Www.

Khalil, M., Amin, M., & Lukiati, B. (2020). *Analisis Potensi Senyawa Repensol Sebagai Kandidat Inhibitor Replikasi Virus Hepatitis B Secara In Silico*. 1–6.

Klebe, G. (2013). Protein–Ligand Interactions As The Basis For Drug Action. *Drug Design*, 61–88. Https://Doi.Org/10.1007/978-3-642-17907-5_4

Lam, T. P., Tran, N. V. N., Pham, L. H. D., Lai, N. V. T., Dang, B. T. N., Truong, N. L. N., Nguyen-Vo, S. K., Hoang, T. L., Mai, T. T., & Tran, T. D. (2024). Flavonoids As Dual-Target Inhibitors Against A-Glucosidase And A-Amylase: A Systematic Review Of In Vitro Studies. *Natural Products And Bioprospecting*, *14*(1). Https://Doi.Org/10.1007/S13659-023-00424-W

Laswati, D. T. (2018). Teh Bunga Kersen (Muntingia Calabura, L): Sifat Kimia Dan Sensoris. *Seminar Nasional Inovasi Produk Pangan Lokal Untuk Mendukung Ketahanan Pangan Universitas Mercu Buana Yogyakarta*, 49–54. Https://Ejurnal.Mercubuana-Yogya.Ac.Id/Index.Php/Prosiding_Ippl/Article/View/705

Mahmood, N. D., Nasir, N. L. M., Rofiee, M. S., Tohid, S. F. M., Ching, S. M., Teh, L. K., Salleh, M. Z., & Zakaria, Z. A. (2014a). Muntingia Calabura: A Review Of Its Traditional Uses, Chemical Properties, And Pharmacological Observations. *Pharmaceutical Biology*, *52*(12), 1598–1623. Https://Doi.Org/10.3109/13880209.2014.908397

Mahmood, N. D., Nasir, N. L. M., Rofiee, M. S., Tohid, S. F. M., Ching, S. M., Teh, L. K., Salleh, M. Z., & Zakaria, Z. A. (2014b). Muntingia Calabura: A Review Of Its Traditional Uses, Chemical Properties, And Pharmacological Observations. *Pharmaceutical Biology*, *52*(12), 1598–1623. Https://Doi.Org/10.3109/13880209.2014.908397

Manna, A., Laksitorini, M. D., Hudiyanti, D., & Siahaan, P. (2017). Molecular Docking Of Interaction Between E-Cadherin Protein And Conformational Structure Of Cyclic Peptide Adtc3 (Ac-Cadtpc-Nh2) Simulated On 20 Ns. *Jurnal Kimia Sains Dan Aplikasi*, *20*(1), 30–36. Https://Doi.Org/10.14710/Jksa.20.1.30-36

Nguyen, H. X., Le, T. M., Le, T. H., Truong, T. Q., Nguyen, B. Q. H., Nguyen, P. T., Le, K. M., Van Do, T. N., Nguyen, M. T. T., Nguyen, M. H., & Nguyen, N. T. (2025). Flavones From Muntingia Calabura Leaves: Structural Elucidation And Sar For A-Glucosidase Inhibition By In Vitro And In Silico Evaluation. *Rsc Advances*, *15*(32), 26444–26454. Https://Doi.Org/10.1039/D5ra01818h

Ogboye, R. M., Patil, R. B., Famuyiwa, S. O., & Faloye, K. O. (2022). Novel A-Amylase And A-Glucosidase Inhibitors From Selected Nigerian Antidiabetic Plants: An In Silico Approach. *Journal Of Biomolecular Structure & Dynamics*, *40*(14), 6340–6349. Https://Doi.Org/10.1080/07391102.2021.1883480

Padhi, S., Nayak, A. K., & Behera, A. (2020). Type Ii Diabetes Mellitus: A Review On Recent Drug Based Therapeutics. *Biomedicine And Pharmacotherapy*, *131*, 110708. Https://Doi.Org/10.1016/J.Biopha.2020.110708

Perkeni. (2015). Panduan Penatalaksanaan Dm Tipe 2 Pada Individu Dewasa. *Panduan Penatalaksanaan Dm Tipe 2 Pada Individu Dewasa Di Bulan Ramadan*, 82. Https://Www.Google.Com/Url?Sa=T&Source=Web&Rct=J&Url=Https://Pbperkeni.Or.Id/Wp-Content/Uploads/2019/01/4.-Konsensus-Pengelolaan-Dan-Pencegahan-Diabetes-Melitus-Tipe-2-Di-Indonesia-Perkeni-2015.Pdf&Ved=2ahukewjy8kos8cfoahxcb30khqb1ck0qfjadegqibhab&Usg=Aov

Pires, D. E. V., Blundell, T. L., & Ascher, D. B. (2015). Pkcsm: Predicting Small-Molecule Pharmacokinetic And Toxicity Properties Using Graph-Based Signatures. *Journal Of*

Medicinal Chemistry, *58*(9), 4066–4072. Https://Doi.Org/10.1021/Acs.Jmedchem.5b00104/Suppl_File/Jm5b00104_Si_001.Pdf

Prayogi, S., Dhiani, B. A., & Djalil, A. D. (2023). Molecular Docking Of Bicycloproline Derivative Synthetic Compounds On Envelope Protein: Anti-Sars-Cov-2 Drug Discovery. *Jurnal Farmasi Dan Ilmu Kefarmasian Indonesia*, *10*(1), 11–21. Https://Doi.Org/10.20473/Jfiki.V10i12023.11-21

Rahmadani, N., Septiani, K. S., Yulianti, R., Handayani, I. S., Haitomi, A., Al-Ghani, M. G., Febrinatasia, W., Murdiyanti, R., Febrinatasia, W., Sulistiyo, R. B., Uthami, M., Rahmi, F., Archi, M., Parura, N. L., Ngenda, F. V., Annida, S. F., Dewi, R. S., Fauzia, S., Ninawati, … Haekal, A. F. (2022). *Tentang Etnobiologi Di Kalimantan Selatan* (Issue March). Cv. Batang.

Rehman, N. U., Rafiq, K., Khan, A., Halim, S. A., Ali, L., Al-Saady, N., Al-Balushi, A. H., Al-Busaidi, H. K., & Al-Harrasi, A. (2019). A-Glucosidase Inhibition And Molecular Docking Studies Of Natural Brominated Metabolites From Marine Macro Brown Alga Dictyopteris Hoytii. *Marine Drugs*, *17*(12), 666. Https://Doi.Org/10.3390/Md17120666

Reuse, A. J. J., & Wisselaar, H. A. (1994). An Evaluation Of The Potential Side-Effects Of A-Glucosidase Inhibitors Used For The Management Of Diabetes Mellitus. *European Journal Of Clinical Investigation*, *24*(S3), 19–24. Https://Doi.Org/10.1111/J.1365-2362.1994.Tb02251.X

Roig-Zamboni, V., Cobucci-Ponzano, B., Iacono, R., Ferrara, M. C., Germany, S., Bourne, Y., Parenti, G., Moracci, M., & Sulzenbacher, G. (2017). Structure Of Human Lysosomal Acid A-Glucosidase-A Guide For The Treatment Of Pompe Disease. *Nature Communications*, *8*(1). Https://Doi.Org/10.1038/S41467-017-01263-3

Sami, F. J., Nur, S., Ramli, N., Sutrisno, B., Tinggi, S., Farmasi Makassar, I., Farmasi, A., & Makassar, K. (2017). Uji Aktivitas Antioksidan Daun Kersen (Muntingia Calabura L.) Dengan Metode Dpph (1,1-Difenil-2-Pikrilhidrazil) Dan Frap (Ferric Reducing Antioxidan Power). *As-Syifaa Jurnal Farmasi*, *9*(2), 106–111. Https://Doi.Org/10.56711/Jifa.V9i2.258

Sari, I. W., Junaidin, J., & Pratiwi, D. (2020). Studi Molecular Docking Senyawa Flavonoid Herba Kumis Kucing (Orthosiphon Stamineus B.) Pada Reseptor A-Glukosidase Sebagai Antidiabetes Tipe 2. *Jurnal Farmagazine*, *7*(2), 54. Https://Doi.Org/10.47653/Farm.V7i2.194

Sinulingga, S., Biokimia, B., Studi Pendidikan Dokter, P., Kedokteran, F., Sriwijaya Jl Moh Ali Komp Rsmh, U., Palembang, K., & Selatan, S. (2020). Uji Fitokimia Dan Potensi Antidiabetes Fraksi Etanol Air Benalu Kersen (Dendrophtoe Petandra (L) Miq). *Jurnal Kedokteran Dan Kesehatan*, *16*(1), 76–83. Https://Doi.Org/10.24853/Jkk.16.1.76-83

Tahir, M., Rahmawati, R., Maryam, S., Nurfauziah, P., & Nazhifah, N. (2022). Aktivitas Senyawa Flavanoid Ekstrak Etanol Bunga Kersen (Muntingia Calabura L) Sebagai Tabir Surya. *As-Syifaa Jurnal Farmasi*, *14*(2), 97–104. Https://Doi.Org/10.56711/Jifa.V14i2.839

Yang, Y., Shi, C.-Y., Xie, J., Dai, J.-H., He, S.-L., & Tian, Y. (2020). Identification Of Potential Dipeptidyl Peptidase (Dpp)-Iv Inhibitors Among Moringa Oleifera Phytochemicals By Virtual Screening, Molecular Docking Analysis, Adme/T Based Prediction, And In Vitro Analyses. *Molecules*, *25*, 189.